

Modelling imaging performance of snake infrared sense

Andreas B. Sichert, Paul Friedel, J. Leo van Hemmen

Abstract. Several snake species use infrared-sensitive pit organs to localise prey. These sensory organs enable the snake to successfully strike prey items even in total darkness or following the disruption of other sensory systems. The pit organ has traditionally been thought to function as a pinhole camera. The need, however, to gather a reasonable amount of thermal energy per time unit (second) necessitates the “pinhole” of the pit organ to be very large, thus greatly reducing its optical performance. Although the image that is formed on the pit membrane has a very low quality, the information that is needed to reconstruct the original temperature distribution in space is still available. In this paper, we present an explicit mathematical model that allows the original heat distribution to be reconstructed from the low-quality image on the membrane.

Introduction

Pit vipers and boids possess infrared (IR) sensitive organs that play an important role in their sensory ecology. Newman and Hartline (Newman and Hartline 1982) suggested that rattlesnakes can strike a heat target with a precision of 5°. Furthermore, the infrared-sensitive pit organs of rattlesnakes project into the *Tectum opticum* forming a spatiotopic map (Newman and Hartline 1981). These findings suggest a considerable spatial resolution of the neuronal image that is formed by the IR organs.

Several snake species have a very high sensitivity to IR radiation detecting temperature differences down to 0.003°C (Bullock and Diecke 1956; for further references see Molenaar 1992). In contrast to the retina, the IR sensing mechanism seems not to be based on a photochemical reaction. Rather, the temperature of the membrane causes the nerve cells to respond (de Cock Buning et al. 1981). In addition, structural specialisation of the periphery containing the receptor cells enhances the sensitivity. Following (Molenaar 1992) we may distinguish three different types of infrared sensitivity in snakes:

1. “*Boa* type” organs: IR-sensitive cells are found on the supra- and infralabial scales, and no specialisation of the scale surface is present;
2. “*Python* type” organs: the sensitive cells are again found supra- and infralabial within grooves formed by the scales;
3. “*Crotalus* type” organs: the heat-sensitive cells lie within a thin (15 µm) membrane that is suspended in the pit organ, lowering the detection threshold; see figure 1.

Only one pit organ is present at each side of the head, whereas in the first two types, multiple IR-sensitive sites may be present at both sides of the head.

The *Python* and *Crotalus* type of sensors are traditionally thought to function as pinhole cameras: an incoming light ray passes through the opening (aperture) of the organ and hits the light-sensitive membrane. The superposition of all incoming light rays then forms an image of the original heat source on the membrane. If the aperture of the organ is very small, the image of a light ray coming from one point is approximately a point. That is, if the opening is small, one point on the membrane corresponds to exactly one point in space outside. If on the other hand the aperture of the organ is large, the image of a point source of heat is disc-shaped rather than point-like. Since, however, the size of the disc-shaped image may be determined by the detectors on the membrane, it is still possible to tell from which direction the radiation comes, ensuring directional sensitivity of the system; cf. figure 1.

The above approach breaks down if the organ is stimulated with real input. Unlike in the laboratory case, point sources of heat are hardly found in nature. Not only do prey animals subtend a significant angle within the view field of the organ, but distraction and noise may be present as well. Several sources of heat then project onto the membrane at the same time and the resulting picture will not at all be disc-shaped. The question we wish to answer in this paper is how the snake may be able to extract information on the location of the prey from the blurred image that is formed on the pit-membrane.

Optical treatment of the problem

To understand the nature of the problem we are dealing with, it is necessary to take a closer look at the input

signals of the IR organs. Any source of heat, such as a prey animal, emits IR radiation. The radiation intensity is distributed over a wide range of wavelengths, the exact profile depending on the surface temperature of the source. Warm objects emit more energy than cool objects and the emitted radiation intensity is concentrated around smaller wavelengths. The radiation emitted by an animal with a surface temperature of 30°C can be described accurately by Planck's law of radiation. We then find that the radiation intensity is maximal for a wavelength of 9.5 μm , which lies

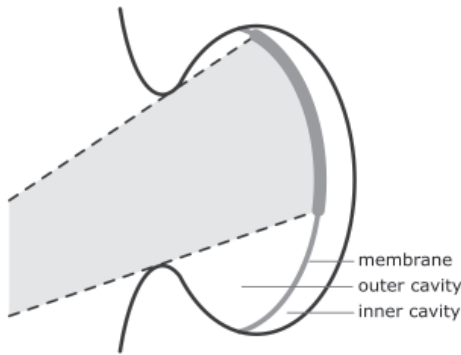


Figure 1. The snake infrared-sensitive pit organ consists of a cavity where a thin membrane containing heat-sensitive nerve receptors is suspended. Because the membrane is suspended, heat reaching the membrane cannot diffuse into adjacent tissue and the membrane is more effectively heated, enhancing the heat sensitivity. An incoming light ray will illuminate a disc shaped region on the membrane. The opening of the organ and its depth measure about 1 mm.

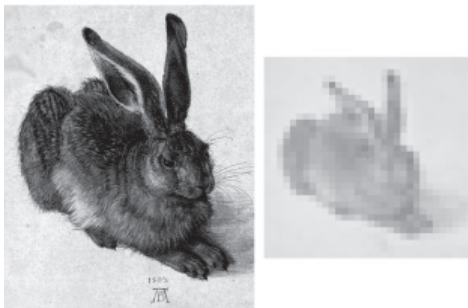


Figure 2. This engraving by the German artist Albrecht Dürer from 1502 (left) has been used as a test for the reconstruction model. The image was converted into an artificial heat distribution, shown on the right. The heat distribution is not biologically realistic. It only serves to demonstrate the capabilities of the proposed model.

exactly within the atmospheric transmission window for far-IR radiation (8-12 μm). Since a typical IR organ measures about 1 mm, the characteristic wavelength of the incoming radiation is much smaller than the organ size and therefore, we may neglect bending and refraction effects as the radiation enters the organ (see e.g. Tipler and Mosca 2004); all light rays entering the organ follow straight lines. This may seem trivial but the condition that the organ size is large compared to the radiation wavelength is not automatically fulfilled for small systems detecting IR radiation and hence should be checked.

As mentioned above, the image on the membrane resulting from the total heat distribution in space will be some complicated shape that consists of the sum, i.e., the superposition of the contributions of all heat sources. This point is made clear in figure 3. We took the famous engraving by Albrecht Dürer depicting a hare and converted this into a “heat intensity profile” (see figure 2). We then calculated the resulting heat distribution on the membrane (see equation 4). In panel A of figure 3, we see what happens for a very small aperture. Since every point in space corresponds to effectively one point (pixel) on the membrane, the heat distribution on the membrane is just a scaled upside-down version of the heat distribution in space. The case is rather different if the aperture of the organ is large. Then, the image on the pit-membrane does not at all look like the original heat distribution (panel B of figure 3).

The obvious question therefore is: Why does the pit organ have such a large aperture? The answer to this question is simple. If the aperture was very small, the amount of energy per unit time (second) reaching the membrane would also be small. This means that the snake would have to wait a long time before enough energy entered the organ to allow for a reliable neuronal response. Even worse, as neuronal integration times are finite, the heat object would hardly ever become observable. So there is a trade-off here. Either the snake ensures that the organ gets strong enough input (large aperture), or the snake forms a sharp image on the membrane (small aperture). Since prey animals are generally moving, it is not an option to wait for enough heat energy to enter the organ. Without the ability of real-time imaging the IR organ would be of little use for the snake.

In the next section, we will argue that it is possible to *reconstruct* the original heat distribution using the blurred image on the membrane. Hence the snake can afford a large aperture organ without losing the important information contained within the signal.

The reconstruction model

We start by presenting the necessary mathematics to gain a minimal understanding of the model. An extensive and mathematically rigorous version of the model has been published elsewhere (Sichert et al. 2006).

Before we can reconstruct the heat distribution in space, we must know the heat image on the pit-membrane. First, we consider the membrane image that is formed when a single point j in real space with intensity \mathbf{O}_j is considered. For the heat intensity at one membrane point i we have

$$(1) \quad \mathbf{I}_i = \mathbf{T}_{ij} \mathbf{O}_j$$

That is, the intensity \mathbf{I}_i at the membrane point i is given by the intensity in space \mathbf{O}_j multiplied by a *transfer function* \mathbf{T}_{ij} . To find the total heat image on the membrane, we must sum the contributions from all points in space,

$$(2) \quad \mathbf{I}_i = \sum_j \mathbf{T}_{ij} \mathbf{O}_j$$

The transfer function describes how effectively heat from a point j can reach the membrane point i . If the point j in space is not visible from the membrane point i (the pathway may be blocked by the organ edge), then there is no heat transfer possible and \mathbf{T}_{ij} vanishes. If the point j is visible, the law of conservation of energy determines the transfer function. The heat reaches the membrane scales with the inverse square distance to the heat source \mathbf{r}_{ij} (since the radiation energy spreads out over a spherical surface area), and with the cosine of the angle ϕ_{ij} . This takes into account that the effective area of the membrane that is “seen” by the incoming radiation is dependent on the incidence angle. We have thus

$$(3) \quad \mathbf{T}_{ij} = \begin{cases} \frac{\cos \phi_{ij}}{|\mathbf{r}_{ij}|^2} & \text{if } j \text{ is visible from } i \\ 0 & \text{otherwise} \end{cases}$$

To include omnipresent noise, we add a stochastic term to the membrane intensity as given by (2) and obtain

$$(4) \quad \mathbf{I}_i = \sum_j \mathbf{T}_{ij} \mathbf{O}_j + \chi_i$$

The variable χ_i has a Gaussian distribution with zero mean and standard deviation σ_{χ_i} . The membrane intensity in (4) is just what the IR sensors on the membrane measure. The next step is trying to reconstruct the *original* spatial heat distribution from the image on the membrane. That is, we try to find a reconstruction, which can be formed from the measure membrane intensity,

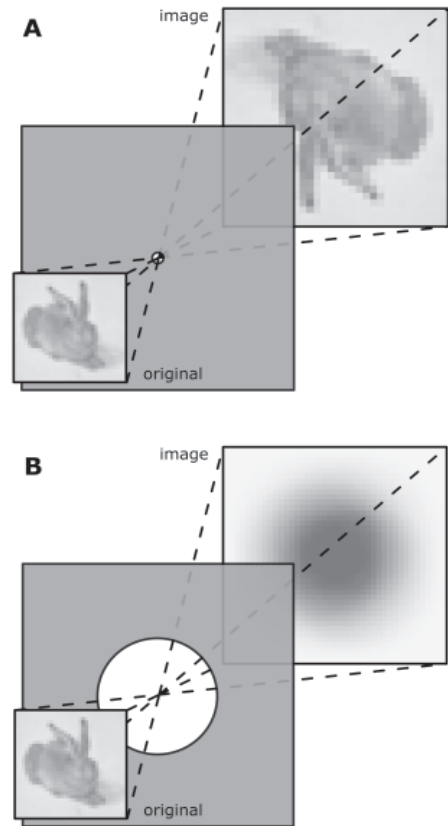


Figure 3. Schematic display of the imaging process. The image chosen here is not biologically realistic. The image only serves to demonstrate the capabilities of our model.

A. If the aperture of the organ is very small, each point in space corresponds to exactly one point on the membrane. Apart from rotation and scaling, the membrane image directly represents the spatial heat distribution.

B. If the aperture is large (comparable in size to the organ depth), the image that is formed on the membrane is blurred. Because light coming from different directions may hit the same point on the membrane, the information content of the spatial heat distribution is smeared out over the membrane.

$$(5) \quad \hat{\mathbf{O}}_j = \sum_i \mathbf{R}_{ji} \mathbf{I}_i$$

The matrix \mathbf{R}_{ij} must now be determined. However, the mapping that was defined in equation (4) has no inverse since some of the information that was present in the original heat distribution is lost and, in addition, equation (4) is of a stochastic nature. The best we can do is to find optimal values for the components of \mathbf{R}_{ij} . We define the error of our estimate (5) as follows,

$$(6) \quad E = \left\langle \sum_i (\hat{O}_i - O_i)^2 \right\rangle$$

To calculate (6), we only have to compute the statistical properties of the input \mathbf{O}_i . The value of \mathbf{O}_i itself need not be known. In our model, we assume that the original heat distribution is totally uncorrelated: knowing the value of \mathbf{O} at any point does not say anything about its value at other points. In reality, the spatial heat distribution will tend to vary smoothly, meaning that neighbouring points in space tend to have heat intensities that are closely alike. We assume, however, that the snake does not “know” this and therefore expects an *a priori* uncorrelated distribution. After reconstruction, the spatial heat distribution may well turn out to be highly structured, as indeed it will in reality often be. In fact, assuming uncorrelated input makes reconstructing the signal *more difficult* and we are dealing with a “worst case scenario”.

We may now calculate the components of the matrix \mathbf{R}_{ij}

to minimise the error (6). Having found the right matrix, we can calculate the “best estimate” of the spatial heat distribution, given the measured heat distribution on the membrane.

Results and discussion

The results of one sample calculation are displayed in figure 4. For the original heat distribution, we used the Dürer picture as in figure 2. The resulting membrane image is shown in figure 4 on the left. The image is severely blurred because the information present in the original heat distribution is distributed over the entire membrane surface. It seems unrealistic that a spatiotopic map could be built using this measured membrane input. On the other hand, after application of equation (5), the image quality is enhanced spectacularly, as shown on the right in figure 4. The original image is clearly recognizable, even in the low resolution that was used in the calculations.

We hope that at this point we made clear that, although the imaging capabilities of the pit-organ are poor, it is still possible to reconstruct the spatial heat distribution. The model we used here is of a mathematical nature. The assumptions that went into the calculations are a “worst case scenario”. For instance, we assumed that the input to the pit organ is totally uncorrelated, meaning that the snake has no idea what heat distribution to expect. In reality, important information about the environment is always available. For example, typical temperature and size of a prey animal may be encoded in the neuronal

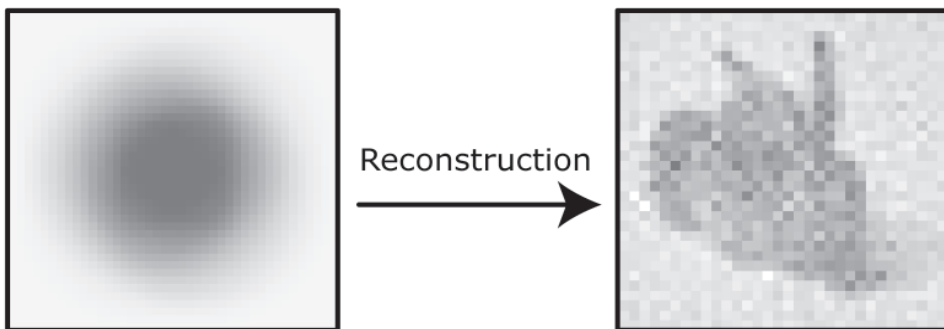


Figure 4. The membrane image on the left still contains enough information to reconstruct the original heat distribution (compare figure 2). The quality of the reconstruction is quite amazing. For computational reasons, the heat distribution and the membrane have been taken as squares, but the model works equally well if applied to a realistic membrane shape. Computational parameters are: organ aperture: 0.8 mm; depth of membrane: 0.86 mm; size of membrane: 1.2 mm x 1.2 mm; number of sensitive cells on the membrane: 41 x 41; spatial heat distribution resolution: 32 x 32 points.

processing structure. If the snake “knows” what kind of images to expect, the reconstruction process can be enhanced considerably.

A neuronal implementation of the model is fairly straightforward. In neuronal terms, the matrix \mathbf{R}_{ij} would correspond to a network of connections between the membrane IR detectors and tectal neurons building the map. The strength of the individual connections would just be the value of the corresponding entry in \mathbf{R}_{ij} . Optimisation of the coefficients in the matrix could be obtained by comparing the information from the IR system with the visual map in the *Tectum opticum*, thus learning the right neuronal connection strengths (see for instance Franosch et al. 2005).

The obvious next step would be to formulate the model in biological terms, using realistic, spiking neurons, realistic input and physical properties of the pit organ. Adding these components to the model would presumably not change the main conclusion of this paper: the information needed for reconstruction is still present in the membrane image.

At present it is not known how accurate the snake IR system really is. It has been shown that the IR system suffices for localising prey without using other sensory input. Furthermore, a tectal map is formed that lies on top of the visual map (Newman and Hartline 1981). These findings suggest that considerable accuracy is indeed possible using the IR sense. We have shown that such accuracy can be obtained using the (low-quality!) imaging hardware that snakes possess, with some basic neuronal processing.

The experiments described in (Newman and Hartline 1982) are highly simplistic. A soldering iron was used as a heat source in experiments measuring the strike accuracy. Being point-like and having a temperature that does not correspond to biological reality, a

soldering iron can hardly be considered as an accurate prey animal model. These experiments therefore cannot be considered as conclusive. Many questions about the IR system still require a truly quantitative answer: What is the striking accuracy if snakes must rely on the IR system *only*? What is the detection range of the IR sense? What is the influence of background noise and distraction? Nevertheless we hope that this paper made a contribution to the interesting debate as to how snake infrared localisation works.

Acknowledgements. The authors thank Guido Westhoff for biological support, Moritz Franosch for fruitful discussions and Bruce Young for critically reading the manuscript. PF was funded by DFG grant HE 3252/3. JLvH was partially founded by the Bernstein Center for Computational Neuroscience.

References

- Bullock, T.H., Diecke, F.P.J. (1956): Properties of an infrared receptor. *J. Physiol. (London)* **134**: 47-87.
- Cock Buning, T. de, Terashima, S., Goris, R.C. (1981): Python pit organs analyzed as warm receptors. *Cell. Mol. Neurobiol.* **1**:271-277.
- Franosch, J.M.P. Lingenheil, M., van Hemmen, J.L. (2005): How a frog can learn what is where in the dark. *Phys. Rev. Lett.* **95**: 078106.
- Molenaar, G. J. (1992): Anatomy and Physiology of Infrared Sensitivity of Snakes. In: *Biology of the Reptilia*, Vol. 17, Sensorimotor Integration, p. 367-453. Gans, C., Ulinski, P.S., Eds, Chicago, University of Chicago Press.
- Newman, E.A., Hartline, P.H. (1981): Integration of visual and infrared information in bimodal neurons of the rattlesnake optic tectum. *Science* **213**: 789-791.
- Newman, E.A., Hartline, P.H. (1982): The infrared “vision” of snakes. *Sci. Am.* **246**(3): 98-107.
- Sichert, A.B., Friedel, P., Hemmen, J. L. van (2006) Snake’s perspective on heat: Reconstruction of input using an imperfect detection system. *Phys. Rev. Lett.* **97**:068105.
- Tipler, P.A., Mosca, G. (2004): *Physics for Scientists and Engineers*, 5th Edition. NY, W.H. Freeman.